



STRUCTURAL  
CHEMISTRY

**Volume 74 (2018)**

**Supporting information for article:**

**Inclusion complex of  $\beta$ -cyclodextrin with coffee chlorogenic acid:  
new insights from a combined crystallographic and theoretical  
study**

**Thammarat Area**

**List of Tables and Figures****Table S1** O–H…O hydrogen bonds in the  $\beta$ -CD–CGA complex from X-ray analysis**Table S2** O–H…O hydrogen bonds in the trimodal  $\beta$ -CD–CGA inclusion complexes from DFT full-geometry optimization**Table S3** O–H…O hydrogen bonds in the dimeric  $\beta$ -CD–CGA inclusion complex from DFT full-geometry optimization**Table S4** Selected geometrical parameters of the four  $\beta$ -CD macrocycles in the  $\beta$ -CD–CGA complexes from X-ray analysis and DFT calculation**Table S5** Stabilization energies of the trimodal and dimeric  $\beta$ -CD–CGA inclusion complexes from DFT full-geometry optimization**Figure S1** Molecular structures of the trimodal  $\beta$ -CD–CGA inclusion complexes from DFT full-geometry optimization in comparison with the starting structures from X-ray analysis**Figure S2** Molecular structure of the dimeric  $\beta$ -CD–CGA inclusion complex from DFT full-geometry optimization in comparison with the starting structure from X-ray analysis**Figure S3** Molecular structures of the trimodal  $\beta$ -CD–CGA inclusion complexes from DFT full-geometry optimization**Figure S4** Molecular structure of the dimeric  $\beta$ -CD–CGA inclusion complex from DFT full-geometry optimization

**Table S1** O–H…O hydrogen bonds in the  $\beta$ -CD–CGA complex from X-ray analysis.

D–H…A	D–H	D…A	D–H…A	D–H…A	D–H	D…A	D–H…A
$\beta$ -CD– $\beta$ -CD			O12W–H1…O34 <sup>ii</sup>	0.96	2.96(1)		154.5
O21–H…O37	0.84	2.795(5)	159.3	O12W–H2…O21 <sup>xiii</sup>	0.95	2.922(9)	147.1
O31–H…O22	0.84	2.864(5)	152.9	O13W–H1…O66	0.96	2.707(6)	148.9
O22–H…O27 <sup>iv c</sup>	0.84	3.001(5)	145.7	O13W–H2…O56 <sup>xiv</sup>	0.96	2.797(5)	156.1
O33–H…O32 <sup>i</sup>	0.84	2.760(5)	168.4	O5W…O23		2.85(3)	
			CGA <sup>a</sup> – $\beta$ -				
O24–H…O10WB <sup>vi b</sup>	0.84	2.85(3)	171.6	CD/CGA/H <sub>2</sub> O			
O34–H…O31 <sup>i</sup>	0.84	2.756(5)	167.4	O1'A–H…O43 <sup>i</sup>	0.84	2.822(9)	127.2
O35–H…O26	0.84	2.900(5)	173.6	O1'B–H…O45 <sup>i</sup>	0.84	2.728(8)	162.8
O65–H…O62 <sup>ix</sup>	0.84	2.706(6)	146.7	O2'–H…O3 <sup>i</sup>	0.84	2.790(6)	142.2
O27–H…O36	0.84	2.880(6)	127.6	O1–H…O64 <sup>ii</sup>	0.84	2.671(5)	167.5
O67–H…O63 <sup>x</sup>	0.84	2.989(5)	174.4	O2–H…O1	0.84	2.732(5)	142.1
$\beta$ -CD–H <sub>2</sub> O			O61–H…O2 <sup>ii</sup>	0.84	2.724(5)		171.3
O32–H…O7W <sup>i</sup>	0.84	2.91(2)	139.0	O2–H…O1W	0.84	2.93(2)	124.0
O23–H…O6W	0.84	2.52(1)	157.9	O3–H…O66	0.84	2.984(5)	166.6
O23–H…O7W	0.84	3.11(2)	167.5	O6–H…O62 <sup>v</sup>	0.84	2.602(6)	137.1
O63–H…O8W	0.84	2.718(6)	150.3	O3W…O1		2.90(1)	
O64–H…O9W	0.84	2.658(7)	160.9	O3W…O5		2.76(1)	
O25–H…O7W <sup>viii</sup>	0.84	2.64(2)	170.4	H <sub>2</sub> O–H <sub>2</sub> O			
O66–H…O9W <sup>ii</sup>	0.84	2.709(6)	156.1	O9W–H1…O1W <sup>vii</sup>	0.96	3.08(2)	145.5
O26–H…O10WA	0.84	2.665(8)	167.0	O9W–H1…O2W <sup>vii</sup>	0.96	2.59(1)	154.2
O26–H…O10WB	0.84	2.99(3)	162.6	O9W–H2…O8W	0.96	2.80(1)	131.7
O36–H…O10WB <sup>i</sup>	0.84	2.66(2)	124.4	O11W–H2…O10WA <sup>xii</sup>	0.96	2.90(1)	129.5
O37–H…O6W <sup>x</sup>	0.84	2.90(1)	136.3	O11W–H2…O10WB <sup>xii</sup>	0.96	2.38(3)	130.6
O37–H…O7W <sup>x</sup>	0.84	2.67(2)	127.6	O1W…O3W		3.05(2)	
O8W–H1…O57 <sup>xi</sup>	0.96	3.121(6)	151.5	O4W…O6W <sup>v</sup>		2.93(2)	
O9W–H2…O54	0.96	2.974(6)	133.5				

<sup>a</sup> Twofold disordered O1'–H group of CGA with occupancy factor 0.5 for both sites A and B.<sup>b</sup> Water sites with occupancy factors: 1.0 (O8W, O9W, O13W); 0.8 (O10WA); 0.7 (O2W, O12W), 0.6 (O3W), 0.5 (O6W, O7W, O11W), 0.4 (O4W), 0.3 (O1W, O5W) and 0.2 (O10WB).<sup>c</sup> Symmetry codes: (i) 1 – x, y, 0.5 – z; (ii) x – 0.5, –y + 0.5, –z + 1; (iii) x – 0.5, y + 0.5, z;

(iv) –x + 0.5, y + 0.5, –z + 0.5; (v) x, –y + 1, –z + 1; (vi) –x + 1.5, y + 0.5, –z + 0.5;

(vii) x + 0.5, –y + 0.5, –z + 1; (viii) –x + 1.5, y – 0.5, –z + 0.5; (ix) x + 0.5, y – 0.5, z; (x) x – 0.5, y – 0.5, z;

(xi) x + 0.5, y + 0.5, z; (xii) –x + 1, –y, z + 0.5; (xiii) –x + 0.5, –y + 0.5, z + 0.5; (xiv) x, –y, –z + 1.

**Table S2** O–H···O hydrogen bonds in the trimodal  $\beta$ -CD–CGA inclusion complexes from DFTfull-geometry optimization [ $\text{\AA}$ ,  $^\circ$ ].<sup>a</sup>

D–H···A	D–H	D···A	D–H···A	D–H···A	D–H	D···A	D–H···A	
<i>Mode 1:</i>								
<i>Bridge</i>								
$\beta$ -CD– $\beta$ -CD		Round		conformation				
O21–H···O37	0.98	3.00	158.9		CGA– $\beta$ -CD			
O31–H···O22	0.98	2.95	166.1		O3–H···O66	0.98	2.89	144.6
O32–H···O23	0.98	2.89	164.4		O66–H···O3'	0.98	2.82	174.1
O33–H···O24	0.98	2.93	163.1					
O34–H···O25	0.98	2.88	166.7					
O35–H···O26	0.98	2.93	166.5					
O27–H···O36	0.98	2.93	152.2					
<i>Mode 2: CFA</i>								
$\beta$ -CD– $\beta$ -CD		Round			CGA– $\beta$ -CD			
O21–H···O37	0.98	2.99	155.3		O66–H···O3'	0.98	2.86	148.2
O31–H···O22	0.98	2.92	165.9					
O32–H···O23	0.98	2.87	165.1					
O33–H···O24	0.98	2.89	165.6					
O25–H···O34	0.98	2.94	144.7					
O35–H···O26	0.98	3.09	167.2					
O27–H···O36	0.98	2.94	151.9					
<i>Mode 3: QNA</i>								
$\beta$ -CD– $\beta$ -CD		Elliptical			CGA– $\beta$ -CD			
O21–H···O37	0.98	2.85	160.5		O1–H···O47	0.99	2.92	155.0
O31–H···O22	0.98	2.94	167.6		O6–H···O42	0.98	2.68	162.0
O32–H···O23	0.98	2.82	168.5		O34–H···O3	0.98	3.00	172.4
O33–H···O24	0.98	2.85	166.1		O37–H···O3'	0.98	2.89	157.9
O25–H···O34	0.98	2.97	168.4					
O35–H···O26	0.98	2.95	172.2					
O27–H···O36	0.98	2.90	144.8					

<sup>a</sup> DFT calculation in vacuum at the B3LYP/6-31+G\*/4-31G level, see also Tables S4 and S5.

**Table S3** O–H···O hydrogen bonds in the dimeric  $\beta$ -CD–CGA inclusion complex from DFT full-geometry optimization [ $\text{\AA}$ ,  $^\circ$ ].<sup>a</sup>

D–H···A	D–H	D···A	D–H···A	D–H···A	D–H	D···A	D–H···A
<i>Monomer 1</i>		$\beta$ -CD	conformation		<i>Monomer 2</i>		
$\beta$ -CD– $\beta$ -CD		Round					
O21–H···O37	0.99	2.87	170.3	O21–H···O37	0.98	2.92	170.2
O31–H···O22	0.99	2.76	164.0	O31–H···O22	0.99	2.75	167.1
O32–H···O23	0.98	2.85	157.5	O32–H···O23	0.98	2.86	160.6
O25–H···O34	0.98	2.89	164.8	O25–H···O34	0.98	2.97	164.1
O35–H···O26	0.99	2.75	168.9	O35–H···O26	0.98	2.89	169.4
O27–H···O36	0.98	2.99	152.8	O27–H···O36	0.98	3.28	134.7
O22–H···O33 <sup>b</sup>	0.98	3.10	156.3	O22–H···O33 <sup>i</sup>	0.98	3.23	147.7
O33–H···O32 <sup>i</sup>	0.98	2.77	178.6	O33–H···O32 <sup>i</sup>	0.99	2.74	175.0
O24–H···O31 <sup>i</sup>	0.97	3.05	120.6	O24–H···O31 <sup>i</sup>	0.97	3.03	120.5
O34–H···O31 <sup>i</sup>	0.99	2.80	162.0	O34–H···O21 <sup>i</sup>	0.99	3.13	121.6
O26–H···O27 <sup>i</sup>	0.99	2.71	162.3	O34–H···O31 <sup>i</sup>	0.99	2.82	159.1
O37–H···O35 <sup>i</sup>	0.99	2.72	166.8	O26–H···O27 <sup>i</sup>	0.98	2.84	156.4
				O37–H···O35 <sup>i</sup>	0.99	2.75	165.0
<i>CGA–<math>\beta</math>-CD/CGA</i>				<i>CGA–<math>\beta</math>-CD/CGA</i>			
O1'–H···O43 <sup>i</sup>	0.98	2.76	140.9	O1'–H···O43 <sup>i</sup>	0.98	2.85	125.9
O66–H···O3' <sup>i</sup>	0.97	2.91	159.3	O66–H···O3' <sup>i</sup>	0.97	2.78	163.4
O2'–H···O3 <sup>i</sup>	0.98	2.80	154.1	O3–H···O66	0.99	2.80	153.7
				O2'–H···O3 <sup>i</sup>	0.98	2.75	149.3

<sup>a</sup> DFT calculation in vacuum at the B3LYP/6-31+G\*/4-31G level, see also Tables S4 and S5.

<sup>b</sup> Atoms belong to the pseudo-twofold symmetry related monomer (i).

**Table S4** Selected geometrical parameters of the four β-CD macrocycles in the β-CD–CGA complexes from X-ray analysis and DFT calculation.

Residue	Tilt angle [°] <sup>a</sup>				O4 angle [°] <sup>b</sup>				O4 deviation [Å] <sup>c</sup>				O4(n)…O4(n – 1), O4(n)…centroid [Å]				
	n	X-ray	Mode 1	Mode 2	Mode 3	X-ray	Mode 1	Mode 2	Mode 3	X-ray	Mode 1	Mode 2	Mode 3	X-ray	Mode 1	Mode 2	Mode 3
1		13.2(1)	7.5	9.9	12.8	128.6(1)	126.6	127.2	118.3	0.119(2)	-0.034	-0.048	0.138	4.372(5)	4.447	4.433	4.530
2		5.2(1)	15.1	10.0	11.2	129.2(1)	128.2	127.0	124.7	0.066(2)	0.263	0.200	0.123	4.333(5)	4.412	4.394	4.144
3		10.6(1)	20.2	16.7	6.6	131.8(1)	131.5	132.4	134.9	0.009(3)	-0.107	-0.094	-0.368	4.345(5)	4.467	4.449	4.567
4		11.0(1)	1.1	0.1	21.7	123.1(1)	125.8	127.8	131.8	0.009(2)	-0.190	-0.099	0.205	4.416(5)	4.391	4.458	4.539
5		9.8(1)	6.6	13.8	16.4	130.9(1)	128.8	124.9	117.1	0.020(3)	0.169	0.079	0.148	4.182(5)	4.398	4.363	4.243
6		18.4(1)	23.2	25.8	10.7	130.6(1)	129.0	131.7	130.1	0.024(3)	0.130	0.107	-0.199	4.594(5)	4.462	4.513	4.346
7		9.5(1)	12.4	12.4	1.9	125.3(1)	128.6	128.2	140.1	0.096(3)	-0.231	-0.145	-0.047	4.257(5)	4.470	4.488	4.572
														5.149	5.104	5.096	4.568
														0.412 <sup>e</sup>	0.079	0.150	0.427
														0.313 <sup>e</sup>	0.208	0.323	1.005
														0.869 <sup>e</sup>	0.869	0.869	0.878

<sup>a</sup> Interplanar angle of the plane through C1(n), C4(n), O4(n) and O4(n – 1) against the O4 plane.<sup>b</sup> O4(n – 1)–O4(n)–O4(n + 1) angle.<sup>c</sup> Deviation of glycosidic O4 atoms from the least-squares plane through the seven O4 atoms.<sup>d</sup> Trimodal β-CD–CGA inclusion complexes derived from DFT energy minimization in vacuum at the B3LYP/6-31+G\*/4-31G level.

Three inclusion modes: mode 1, bridging C=C–C(=O)O group; mode 2, CFA moiety; and mode 3, QNA moiety.

<sup>e</sup> Ranges of the O4(n)…O4(n – 1), O4(n)…centroid distances and the average of their ratios are in *italics*.

1 **Table S5** Stabilization energies of the trimodal and dimeric  $\beta$ -CD–CGA inclusion complexes from  
 2 DFT full-geometry optimization.<sup>a</sup>

	<i>Dimer</i>	<i>Trimodal</i>		
		<i>Mode 1: Bridge</i>	<i>Mode 2: CFA</i>	<i>Mode 3: QNA</i>
<b>DFT calculation</b>				
$E_{\text{cpx}}$ <sup>b</sup>	<b>-11139.50994</b>	-5569.72645	-5569.70310	-5569.70652
$E_{\beta\text{-CD}_\text{opt}}$	<b>-8545.98608</b>	-4272.96989	-4272.95905	-4272.95905
$E_{\text{CGA}_\text{opt}}$	<b>-2593.49283</b>	-1296.72905	-1296.72905	-1296.72905
$\Delta E_{\text{stb}}$ [Hartree] <sup>c</sup>	<b>-0.03103</b>	-0.02751	-0.01500	-0.01842
$\Delta E_{\text{stb}}$ [kcal mol <sup>-1</sup> ]	<b>-19.47</b>	-17.26	-9.42	-11.56
No. of host-guest OH···O H-bonds	<b>5</b>	2	1	4
<b>Experiments</b>				
$\Delta H_{\text{UV}}$ [3–37°C, pH 6.5] <sup>d</sup>	<b>UV</b>			-2.73
$K_{\text{UV}}$ [25°C, pH 6.5] <sup>d</sup>	<b>UV</b>			597±27
$\Delta H_{\text{UV}}$ [5–25°C, pH 6.7] <sup>e</sup>	<b>UV</b>			-6.53±0.93
$K_{\text{UV}}$ [20°C, pH 6.7] <sup>e</sup>	<b>UV</b>			1032±54
$\Delta H_{\text{ITC}}$ [10–55°C, pH 6.7] <sup>f</sup>	<b>Calorimetry</b>			-3.02±0.06
$K_{\text{ITC}}$ [25°C, pH 6.7] <sup>f</sup>	<b>Calorimetry</b>			1467±89
$K_{\text{Fluor}}$ [25°C, pH 7] <sup>g</sup>	<b>Fluorometry</b>	[420±50] <sup>h</sup>		
$\Delta H_{\text{Fluor}}$ [5–25°C, pH 5] <sup>i</sup>	<b>Fluorometry</b>	[-6.10] <sup>h</sup>		
$K_{\text{Fluor}}$ [25°C, pH 5] <sup>i</sup>	<b>Fluorometry</b>	[351±69] <sup>h</sup>	220	93
$\Delta H_{\text{ITC}}$ [5–25°C, pH 5] <sup>i</sup>	<b>Calorimetry</b>	[-3.09] <sup>h</sup>		
$K_{\text{ITC}}$ [25°C, pH 5] <sup>i</sup>	<b>Calorimetry</b>	[442] <sup>h</sup>	207	235
$\Delta H_{\text{Fluor}}$ [5–60°C, pH 7] <sup>j</sup>	<b>Fluorometry</b>			-3.04
$K_{\text{Fluor}}$ [20°C, pH 7] <sup>j</sup>	<b>Fluorometry</b>			424
$K_{\text{NMR}}$ [25°C, pH 7] <sup>k</sup>	<b>NMR</b>			504

<sup>a</sup> DFT/B3LYP calculation using mixed basis sets 4-31G for C atoms and 6-31+G\* for H and O atoms.

X-ray-derived structure was used as a starting model, see also Tables S2 and S3.

Bimodal  $\beta$ -CD–CGA inclusion complex (modes 2 and 3) stems from fluorescence and colorimetric data (Álvarez-Parrilla *et al.*, 2010).

<sup>b</sup> Original unit of  $E$  is Hartree (1 H = 627.5 kcal mol<sup>-1</sup>).

<sup>c</sup> Stabilization energy,  $\Delta E_{\text{stb}} = E_{\text{cpx}} - (E_{\beta\text{-CD}_\text{opt}} + E_{\text{CGA}_\text{opt}})$ , where  $E_{\text{cpx}}$ ,  $E_{\beta\text{-CD}_\text{opt}}$  and  $E_{\text{CGA}_\text{opt}}$  are the energies from full optimization of complex,  $\beta$ -CD and CGA, respectively.

<sup>d</sup> Multiple-temperature UV studies (3–37°C) in aqueous solution. Inclusion structure is predicted using NMR (Irwin *et al.*, 1994). Units:  $\Delta H$ , kcal mol<sup>-1</sup> and  $K$ , M<sup>-1</sup>.

<sup>e</sup> Multiple-temperature UV studies (5–25°C) in MeOH aqueous solution. Inclusion structure is predicted using NMR (Irwin *et al.*, 1995).

<sup>f</sup> Variable-temperature isothermal titration calorimetry (ITC) (10–55°C) in aqueous solution. Inclusion structure is predicted using NMR (Irwin *et al.*, 1999).

<sup>g</sup> Fluorescence data at 25°C, pH 7 (Álvarez-Parrilla *et al.*, 2005).

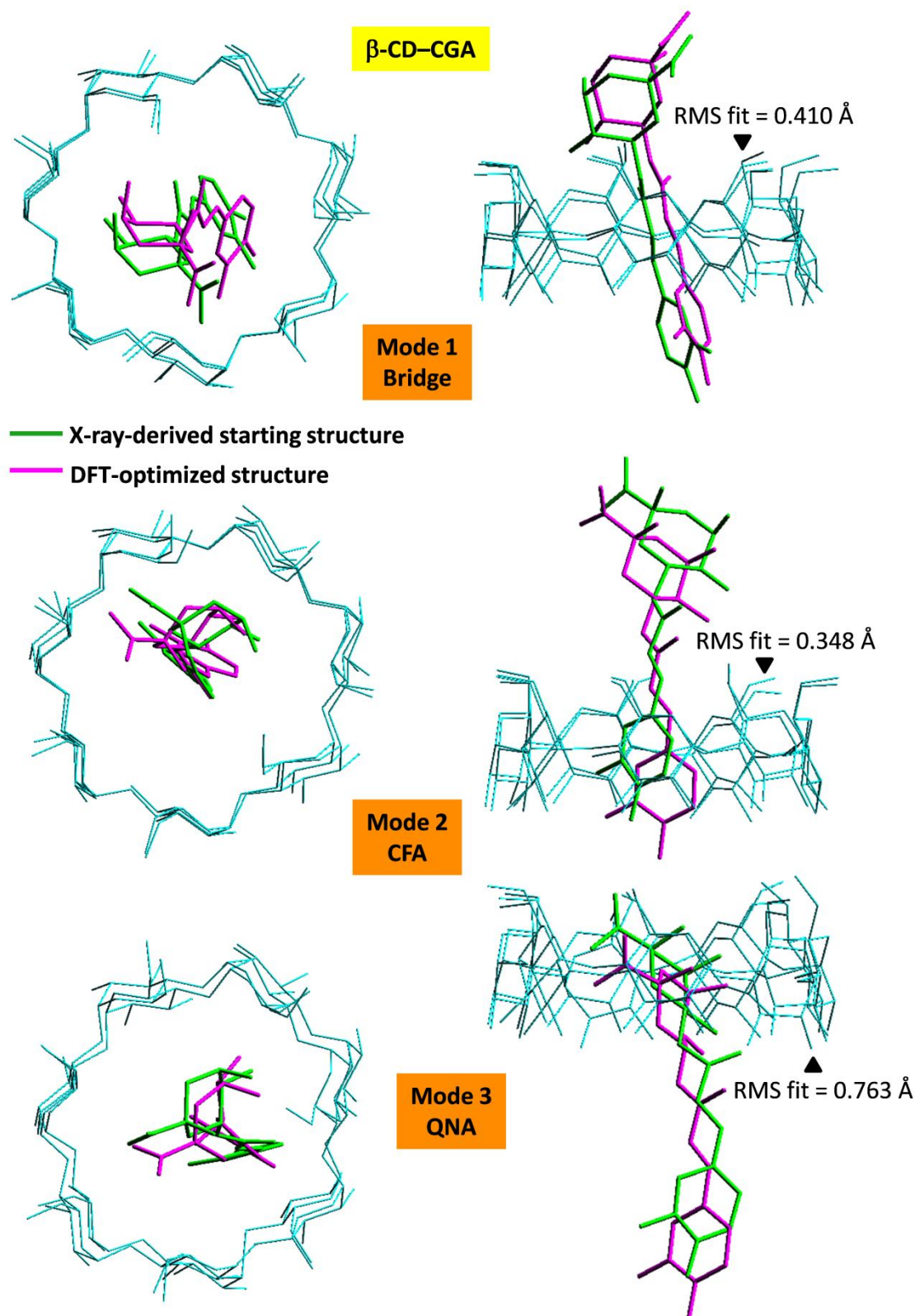
<sup>h</sup> [Macroscopic value] is deduced from two microscopic contributions of the two main structural components of CGA, i.e., CFA and QNA moieties.

<sup>i</sup> Variable-temperature fluorescence and isothermal titration calorimetry (ITC) (5–25°C, pH 5) in aqueous solution. Inclusion structures are predicted using ROESY NMR (Álvarez-Parrilla *et al.*, 2010).

<sup>j</sup> Multiple-temperature fluorescence studies (5–60°C) in aqueous solution.

Inclusion structures are predicted using molecular dynamics (Górnas *et al.*, 2009).

<sup>k</sup> NMR data at 25°C, pH 7 (Rodrigues *et al.*, 2002).



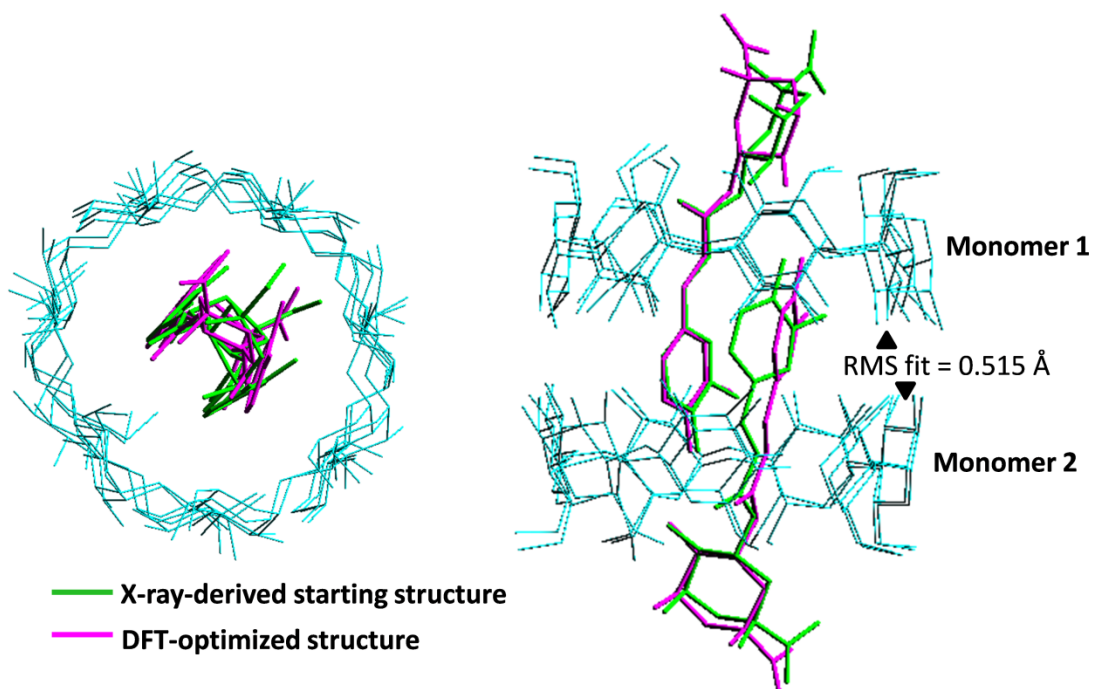
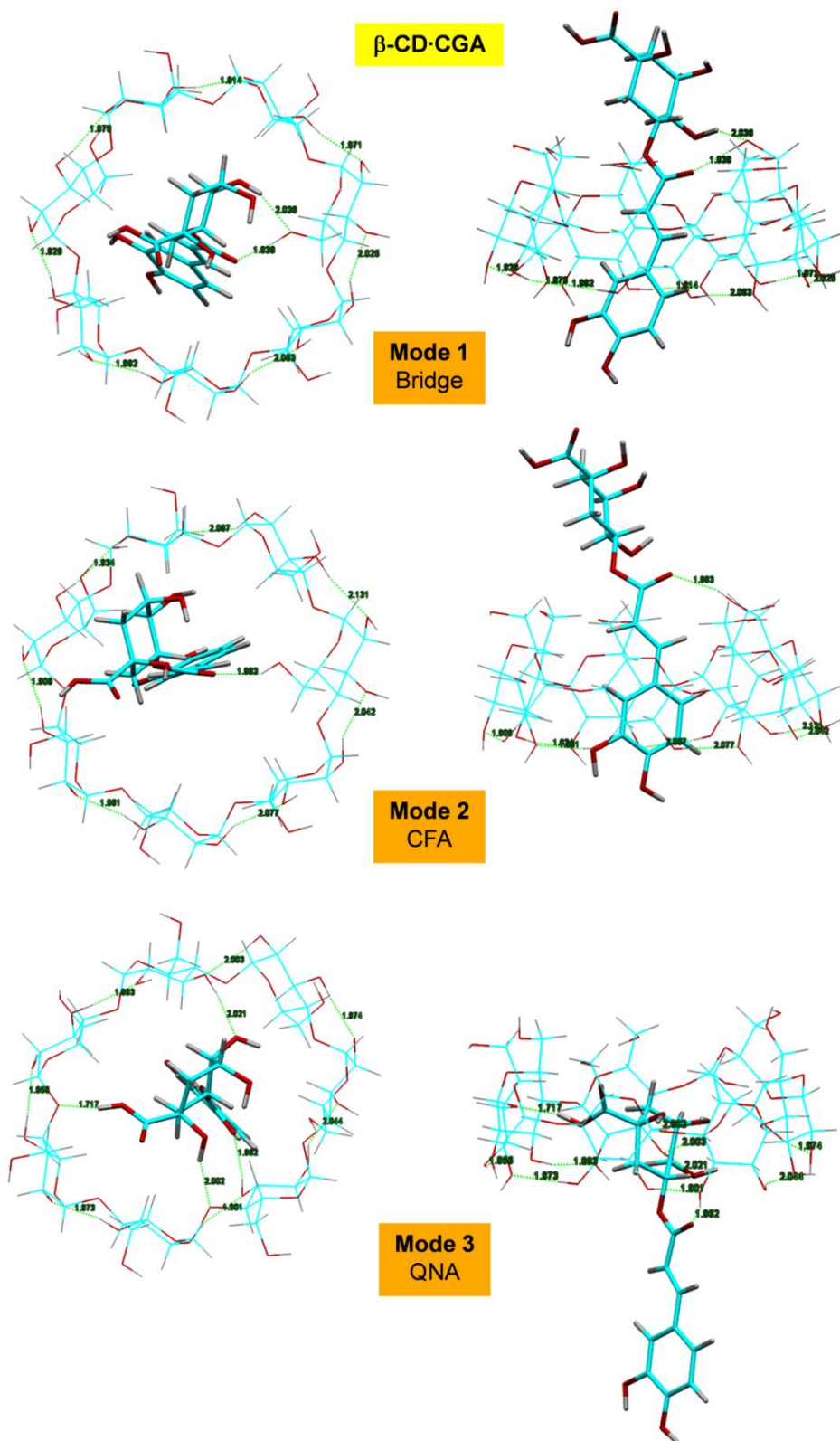
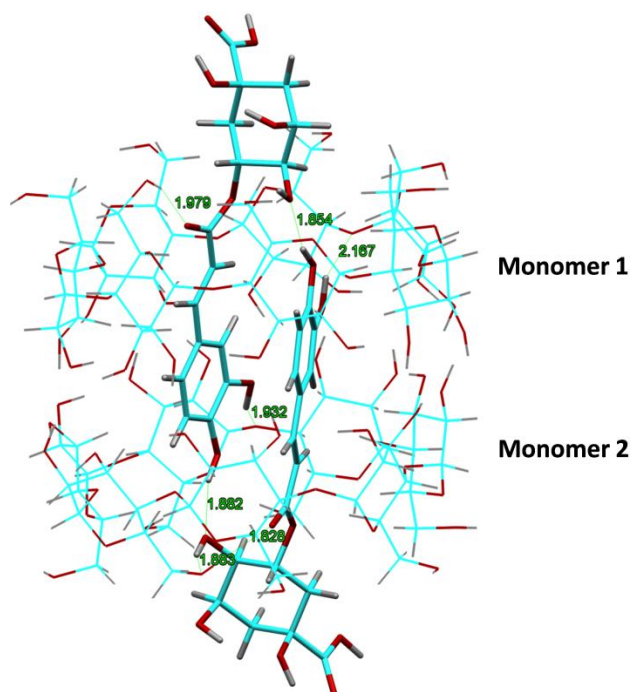


Figure S2 Molecular structure of the dimeric  $\beta$ -CD–CGA inclusion complex from DFT full-geometry optimization in comparison with the starting structure from X-ray analysis; top view (left) and side view (right). RMS fit is calculated for the dimeric  $\beta$ -CD (cyan wireframes), excluding O6, H atoms and guest molecules.



1

2 **Figure S3** Molecular structures of the trimodal  $\beta$ -CD–CGA inclusion complexes from DFT full-  
3 geometry optimization; top view (left) and side view (right). O–H $\cdots$ O hydrogen bonds are indicated by  
4 dotted lines with H $\cdots$ O distances in Å.



1  
2 **Figure S4** Molecular structure of the dimeric  $\beta$ -CD–CGA inclusion complex from DFT full-  
3 geometry optimization. O–H $\cdots$ O hydrogen bonds are indicated by dotted lines with H $\cdots$ O distances in  
4 Å.